

Optimal Sizing and Setting of Distributed Power Condition Controller in Isolated Multi-Microgrid

Mehran Esmaili*; Hossein Shayeghi**†; Khalil Valipour*; Amin Safari**; Farzad Sedaghati*

*Department of Electrical Engineering, University of Mohaghegh Ardabili, Ardabil, Iran

**Department of Electrical Engineering, Azarbaijan Shahid Madani University, Tabriz, Iran

(m.esmaili@uma.ac.ir, hshayeghi@gmail.com, kh_valipour@uma.ac.ir, safari@azaruniv.ac.ir, farzad.sedaghati@uma.ac.ir)

†

Corresponding Author; Hossein Shayeghi, Department of Technical Engineering, University of Mohaghegh Ardabili, Ardabil, Iran, Tel: +98 045 33512910, hshayeghi@gmail.com

Received: 18.06.2020 Accepted: 14.07.2020

Abstract- In the present research, optimal placement and parameter tuning of an improved custom power device called Distributed power condition controller (DPCC) for enhancing the voltage profile and reducing losses in an isolated multi-microgrid (MMG) under critical situations have been investigated. The relative capacity credit of the intermittent renewable sources is typically 25–50 percent. When a critical situation such as generation reduction, DG outage in each MG, overload or line contingency occurs in the MMG, the voltages at some buses fluctuate more than the allowed level and power losses arise which is harmful to vital applications. In this paper, the butterfly optimization algorithm and grasshopper optimization algorithm are suggested to search the optimal placement and parameter tuning of DPCC for enhancing the voltage profile and reducing losses under critical situations. A modified IEEE 33-bus network with four distributed generation is employed to create a sample isolated MMG. Eleven different case studies in seven scenarios are considered to evaluate the high capability of DPCC in regulating voltage and reduce losses. It is found from theory studies and simulation results that optimal placement and parameter tuning of DPCC successfully improve the MMG performance.

Keywords- Butterfly optimization algorithm (BOA), Distributed power condition controller (DPCC), Grasshopper optimization algorithm (GOA), Multi-microgrid, Power loss, Renewable energy sources, Voltage regulation

NOMENCLATURE

Symbols	Continue
B_{ij}	Imaginary part of the (i, j) th entry of admittance matrix
B_{ji}	Imaginary part of the (j, i) th entry of admittance matrix
c	Decreasing factor
c_b	Sensory modality
d_{ij}	Distance between i th and j th grasshopper
f	Perceived magnitude of the fragrance
f_g	The strength of attraction
S_j	Injected apparent power at bus j
t	Current iteration
\hat{T}_d	Best solution in the d th dimension
ub_d	Upper bound in the d th dimension
V_i	The voltage at bus i
V_j	The voltage at bus j
V_{sh}	Controllable magnitude of the voltage source representing the shunt converter

parameter tuning of APF has been investigated for enhancing power quality in the distribution network in the presence of nonlinear load [16]. Based on the obtained results with the grey wolf optimization method, nonlinear loads and DGs affected the location and size of APF. The voltage quality of the smart grid was improved with a new custom power device (CPD) in [17]. The particle swarm optimization (PSO) algorithm was used for the optimal location and tuning of CPDs for minimization of the total CPD injected currents and the total harmonic distortion (THD) of current and voltage. Hence, the real-time control of reactive power with CPD was suggested. The PSO method was proposed to determine the optimal size and location of the distributed active filter system for reducing total losses while satisfying harmonic voltages, THD limits on a typical 37-bus the distribution system [18]. In [19] optimal location of UPQC for enhancing the power quality in the distribution network under critical situations has been investigated. Cuckoo Optimization Algorithm is proposed to find the optimal placement and number of UPQCs for improving the power quality issues. Distributed power condition controller (DPCC) with the fuzzy based PI controller was proposed in [20] to enhance power quality in a multi-microgrid.

The relative capacity credit of renewable power plants is typically 25-50 percent. The intermittent renewable sources and loads in MMG cause many adverse impacts in these networks. In this paper, optimal placement and parameter tuning of DPCC for enhancing the voltage profile and reducing losses in a sample MMG under critical situations with two high-performing optimization algorithms have been investigated. Also, the power injection model of the DPCC for power flow studies has been presented. Butterfly optimization algorithm (BOA) and grasshopper optimization algorithm (GOA) are suggested to search the optimal placement and parameter tuning of DPCC for enhancing the voltage profile and reducing losses which is harmful to vital applications. The proposed method is applied to a modified IEEE 33-bus network which is employed to create a sample isolated MMG. Four DG units are used to create an MMG. In order to evaluate the proposed model, eleven different case studies in seven scenarios are considered. The main contributions of this research are:

- Showing the high capability of DPCC to control bus voltages and reduce losses in the MMG considering capacity credit of the renewable power plants.
- Optimal location and parameter setting of the DPCC for improving the voltage profile and reduce losses in the MMG with two high-performing optimization algorithms.

The rest of the paper is organized as follows: the DPCC model formulation is explained in detailed in Section 2. Section 3 explains the step-by-step the optimization algorithms in the form of the flowchart. The brief explanation of the studied isolated MMG and the simulation results are given in Section 4. Finally, the conclusion is presented in section 5.

2. DPCC MODEL FORMULATION

The power injection model of the DPCC is used in the power flow analysis. The equivalent model of DPCC is presented in Fig. 1.

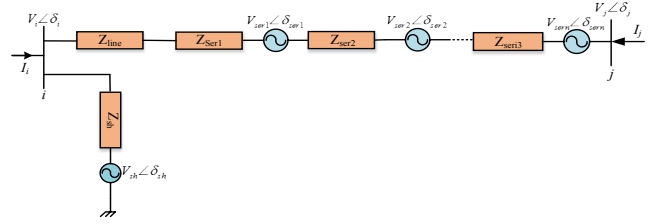


Figure 1. DPCC equivalent circuit

The injected active and reactive power in DPCC as shown in Fig. 2 can be calculated as follows:

$$\begin{bmatrix} P_{is} + Q_{is} \\ P_{js} + Q_{js} \end{bmatrix} = \begin{bmatrix} V_i & 0 \\ 0 & V_j \end{bmatrix} \begin{bmatrix} I_i^* \\ I_j^* \end{bmatrix} \quad (1)$$

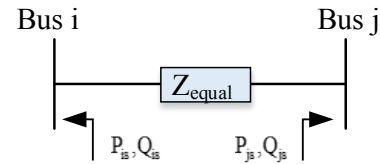


Figure 2. Power injection model of DPCC

The current at bus i and j considering the equivalent model shown in Fig. 1 is given by Eq. (2).

$$\begin{bmatrix} I_i \\ I_j \end{bmatrix} = \begin{bmatrix} Y_{sh} + Y_{ser} & -Y_{ser} & -Y_{ser} & -Y_{sh} \\ -Y_{ser} & Y_{ser} & Y_{ser} & 0 \end{bmatrix} \begin{bmatrix} V_i \\ V_j \\ \sum_{k=1}^n V_{serk} \\ V_{sh} \end{bmatrix} \quad (2)$$

Where Y_{ser} is defined by Eq. (3).

$$Y_{ser} = \sum_{k=1}^n Y_{serk} + Y_{Line} \quad (3)$$

By substituting Eq. (2) in Eq. (1), the injected active and reactive power of the DPCC used in the simulation with the power flow analysis can be expressed as follows:

$$\begin{aligned} P_{is} = & |V_i|^2 G_{ii} + |V_i| |V_j| \{G_{ij} \cos(\delta_i - \delta_j) + B_{ij} \sin(\delta_i - \delta_j)\} \\ & + |V_i| \left| \sum_{k=1}^n |V_{serk}| \{G_{ij} \cos(\delta_i - \delta_{serk}) + B_{ij} \sin(\delta_i - \delta_{serk})\} \right. \\ & \left. + |V_i| |V_{sh}| \{G_{io} \cos(\delta_i - \delta_{sh}) + B_{io} \sin(\delta_i - \delta_{sh})\} \right. \end{aligned} \quad (4)$$

$$\begin{aligned} Q_{is} = & -|V_i|^2 B_{ii} + |V_i| |V_j| \{G_{ij} \sin(\delta_i - \delta_j) + B_{ij} \cos(\delta_i - \delta_j)\} \\ & + |V_i| \left| \sum_{k=1}^n |V_{serk}| \{G_{ij} \sin(\delta_i - \delta_{serk}) - B_{ij} \cos(\delta_i - \delta_{serk})\} \right. \\ & \left. + |V_i| |V_{sh}| \{G_{io} \sin(\delta_i - \delta_{sh}) - B_{io} \cos(\delta_i - \delta_{sh})\} \right. \end{aligned} \quad (5)$$

(6)

$$\begin{aligned}
P_{js} &= |V_j|^2 G_{jj} + |V_j| |V_i| \{G_{ji} \cos(\delta_j - \delta_i) + B_{ji} \sin(\delta_j - \delta_i)\} \\
&+ |V_j| \sum_{k=1}^n (|V_{serk}| \{G_{jj} \cos(\delta_j - \delta_{serk}) + B_{jj} \sin(\delta_j - \delta_{serk})\}) \\
Q_{js} &= -|V_j|^2 B_{jj} + |V_j| |V_i| \{G_{ji} \sin(\delta_j - \delta_i) - B_{ji} \cos(\delta_j - \delta_i)\} \\
&+ |V_j| \sum_{k=1}^n (|V_{serk}| \{G_{jj} \sin(\delta_j - \delta_{serk}) - B_{jj} \cos(\delta_j - \delta_{serk})\})
\end{aligned} \quad (7)$$

3. Optimization Algorithms

Nature-inspired meta-heuristic algorithms have been known as powerful global optimization techniques in recent literatures [21, 22]. BOA and GOA are new meta-heuristic algorithms inspired by the swarming behavior of insects. Some of the main advantages of these algorithms are suitable for global optimization, local optimal avoidance, suitable convergence rate and gradient-free mechanism. Considering these advantages, these two high-performing optimization algorithms are applied for optimal placement and parameter tuning of DPCC for enhancing the voltage profile and reducing losses under critical situations.

3.1. BOA

Within BOA, butterflies are the searching agents performing the optimization. Each butterfly is supposed to generate some intensity fragrance, sensed and propagated by other butterflies in the area. There is a correlation between the fragrance emitted by the butterfly and its fitness. This indicates that altering the position by a butterfly, its fragrance/fitness will accordingly change. When other butterfly's higher fragrance is sensed by a butterfly in the area, the considered butterfly will travel toward the latter butterfly. This stage is named the global search. Within another situation, if a butterfly can't sense fragrance higher than its fragrance, it will randomly move, hence, this stage is named the local search. The entire notion of processing and sensing the modality is oriented by three critical terms called sensory modality (c_b), stimulus intensity (I) and power exponent (a). The sensory modality is the perception associated with the measurement of the type of energy and its processing. The physical/actual stimulus' magnitude is the stimulus intensity [21]. These concepts are used in BOA to formulate the fragrance as a function of the stimulus physical intensity as follows:

$$f = c_b I^a \quad (8)$$

There are two key phases in the BOA, i.e., global and local search steps. In the global search phase, the algorithm is mathematically modeled with Eq. (9), where the position of the i th butterfly can be defined as:

$$x_i^{t+1} = x_i^t + (r^2 \times g^* - x_i^t) \times f_i \quad (9)$$

And, the local search phase can be represented as Eq. (10):

$$x_i^{t+1} = x_i^t + (r^2 \times x_i^t - x_i^t) \times f_i \quad (10)$$

where x_j^t and x_k^t are j th and k th butterflies chosen randomly from the solution space. Where r is a random number between [0, 1]. Considering physical proximity and various other factors like rain, wind, etc., search for food can have a significant fraction p in an overall mating partner or food searching activities of butterflies. So a switch probability p is applied to switch between the global search to local one. The BOA parameters used in the simulation are $N_b = 100$, $p = 0.8, 0.1$, $cb = 0.01$, $\max \text{ iter} = 50$. The step by step method to find the optimal placement and parameter tuning of DPCC using BOA is shown in Fig. 3.

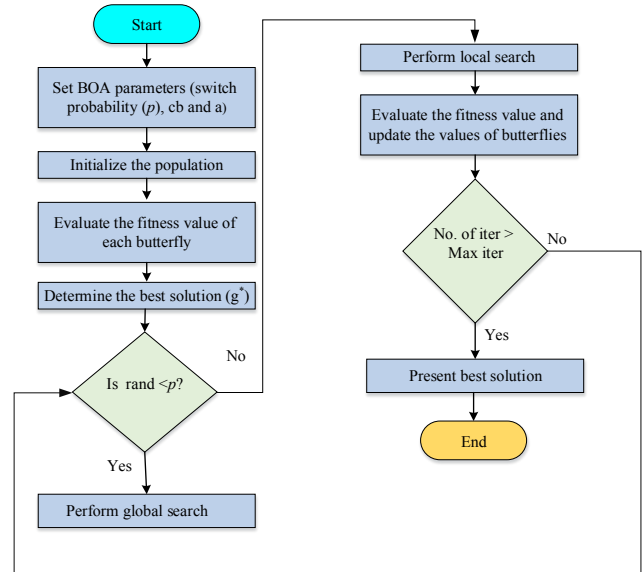


Figure 3. BOA flowchart for optimal location and parameter setting of DPCC in the MMG

3.2. GOA

GOA is a high-performing optimization algorithm stimulated by the grasshoppers' swarming performance. Two opposite forces exist between the grasshoppers, repulsion, and attraction. By the repulsion forces, the grasshoppers are enabled to discover the searching space (global search), promising areas are used by the attraction forces (local search). The area where the two forces are identical is named the comfort zone. The closest position to the target is the grasshoppers' position with the best fitness function; hence, the rests attempt to travel toward the location through network interaction over the iterative stages; the comfort area is adaptively reduced until obtaining the best solution [22].

The proposed algorithm is mathematically modeled with Eq. (11), where the d th dimensional location of the i th grasshopper can be defined as:

$$\begin{aligned}
X_i^d(t+1) = & \\
& c \left[\sum_{i=1}^N c \frac{ub_d - lb_d}{2} s \left(\left| x_j^d(t) - x_i^d(t) \right| \right) \frac{x_j(t) - x_i(t)}{d_{ij}} \right] + \hat{T}_d \quad (11)
\end{aligned}$$

Where, the s function is defined as the strength of social forces, which can be calculated as follows:

$$s(r) = f_g e^{-\frac{r_g}{l_s}} - e^{-r_g} \quad (12)$$

In Eq (11), the current grasshopper location is represented by the part into the bracket based on other grasshoppers in the area and \hat{T}_d shows the agent's movements around the target. Using the first c from the left, the exploration and exploitation of the total grasshopper swarm are balanced around the best global optimal solution. Using the second c , the range of comfort zone, attraction zone, and an exclusion zone is gradually shrunk. The main controlling parameter in the GOA algorithm is the parameter c , which is determined with Eq. (13):

$$c = c_{max} - t \frac{c_{max} - c_{min}}{t_{max}} \quad (13)$$

The parameter c is linearly decreased from 1 to 0 over the course of iterations. These features lead to observe the convergence quickly without getting trapped to local optimum. The GOA parameters used in the simulation are $Ng = 100$, $c_{max} = 1$, $c_{min} = 0.00004$, $t_{max} = 50$. The step by step method to find the optimal placement and parameter tuning of DPCC using GOA is shown in Fig. 4.

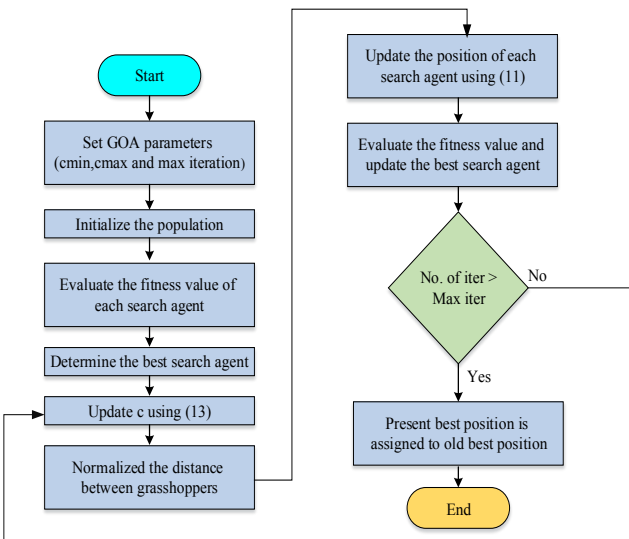


Figure 4. GOA flowchart for optimal location and parameter setting of DPCC in the MMG

4. Simulation results and discussions

4.1. Case study

The proposed method is applied to a modified IEEE 33-bus network which is employed to create a sample isolated MMG [23]. Figure 5 shows a single line diagram of the studied island MMG. The total load of the MMG is 3715 kW+j2300 kVA, and four DG units are used to create an MMG. The specifications of MGs in the studied MMG are presented in Table 1.

Table 1. The specifications of MGs in the studied MMG

MGs	DG capacity		Total load	
	kW	kVAR	kW	kVAR
MG1	1280	1560	1280	1560
MG2	220	460	220	460
MG3	490	1020	490	1020
MG4	310	675	310	675

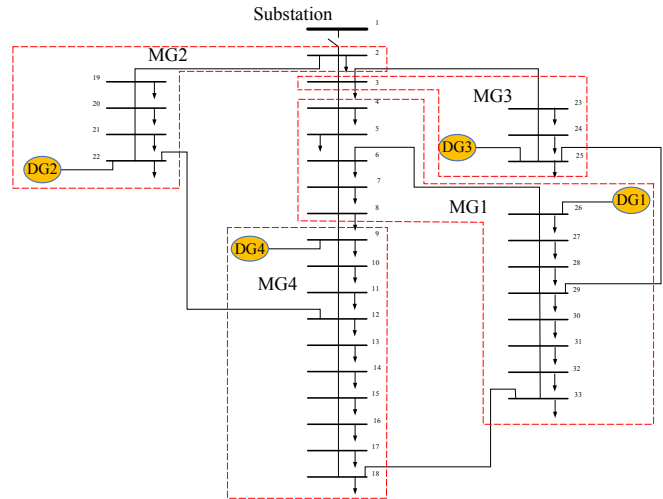


Figure 5. Single-line diagram of the studied MMG

4.2. Objective function

The improvement voltage profile and minimizing the real power losses are considered the two objective functions that can be expressed as follows:

$$F_1 = \sum_{i=1}^{Nb} (V_i - V_{rated})^2 \quad (14)$$

$$F_2 = P_{Loss} = 0.5 \times \sum_{i=1}^{NI} G_i \times \left[|V_i|^2 + |V_j|^2 - 2|V_i||V_j|\cos(\delta_i - \delta_j - \theta_{ij}) \right] \quad (15)$$

And the fitness function can be defined in Eq. (16)

$$\text{Min } F = pf * F_1 + F_2 \quad (16)$$

Where, pf is the weighting factor of voltage deviation. The limitation of buses voltage and power flow equations have been considered as the constraints of the objective function as follows:

$$V_{min} \leq V_{bus} \leq V_{max} \quad (17)$$

$$P_i + P_{DG_i} - P_{LI} - V_i \sum_{l=1}^{Nb-1} V_l \left[G_{ij} \cos(\theta_{ij}) + B_{ij} \sin(\theta_{ij}) \right] = 0 \quad (18)$$

$$Q_i + Q_{DG_i} - Q_{LI} - V_i \sum_{l=1}^{Nb-1} V_l \left[G_{ij} \sin(\theta_{ij}) + B_{ij} \cos(\theta_{ij}) \right] = 0 \quad (19)$$

4.3. Simulation results

To demonstrate the applicability of the DPCC for voltage control and loss reduction in the isolated MMG, different

critical situations were applied to the studied MMG according to Table 2.

Scenario 7: line contingency	Case 11: line 12-22 outage
---------------------------------	----------------------------

For each case in Table 2, two optimization techniques have been employed to find the optimal placement and parameter tuning of the DPCC to minimize the loss and voltage deviation. The five same series converters are used in the DPCC for avoiding unnecessary simulation complexity. The optimization variables are considered as follows:

- (a) The DPCC site in the MMG.
- (b) The series voltage ($0.01 \leq V_{ser} \leq 0.1$).
- (c) The shunt voltage ($0.9 \leq V_{sh} \leq 1.05$).

The optimal placement and parameters of DPCC for different case studies are shown in table 3. Table 4 compares the objective function before and after using DPCC with optimized parameter in the optimized location obtained by the applied techniques. Table 4 shows the negative impacts of various critical scenarios on the MMG can be solved by using DPCC. Figure 6 compares the losses before and after using DPCC for different cases.

Table 2. Different studied cases

Scenarios	Case studies description
Scenario 1: Normal condition	Case 1: Normal condition
Scenario 2: Generation reduction in each MG	Case 2: 50% generation reduction in DG1
Scenario 3: DG outage in each MG	Case 3: DG1 outage
	Case 4: DG2 outage
	Case 5: DG3 outage
	Case 6: DG4 outage
Scenario 4: Overload in each MG	Case 7: 50% overload in MG1
	Case 8: 50% overload in MG4
Scenario 5: Generation reduction in MMG	Case 9: 40% generation reduction
Scenario 6: Overload in MMG	Case 10: 40% overload

Table 3. Optimal placement and parameter tuning of DPCC obtained by BOA and GOA

Case studies	Optimal location of DPCC				Parameter setting of DPCC			
	BOA		GOA		BOA		GOA	
	From bus	To bus	From bus	To bus	V_{ser}	V_{sh}	V_{ser}	V_{sh}
Case 1	27	28	27	28	0.03689	1.0271	0.03641	0.9484
Case 2	27	28	27	28	0.03656	0.9845	0.03642	0.95767
Case 3	23	24	23	24	0.03642	0.9571	0.03669	1.0058
Case 4	27	28	27	28	0.03669	1.0058	0.03626	0.9087
Case 5	27	28	6	7	0.03649	0.9712	0.03621	0.9
Case 6	27	28	27	28	0.03643	0.9599	0.03645	0.9622
Case 7	5	6	27	28	0.03673	1.0107	0.03644	0.9621
Case 8	27	28	27	28	0.0364	0.9523	0.03651	0.9751
Case 9	29	30	29	30	0.03637	0.9443	0.03644	0.9609
Case 10	27	28	5	6	0.03652	0.977	0.03622	0.9
Case 11	27	28	5	6	0.0364	0.9345	0.03627	0.9177

Table 4. Calculated objective functions by BOA and GOA approaches

$pf = 0.01$	Without DPCC		Objective function			
	$F1$	$F2$	BOA		GOA	
			$F1$	$F2$	$F1$	$F2$
Case 1	0.2850	42	6.2e-5	18.4	5.9e-4	21.3
Case 2	0.2883	65	4.3e-7	31.7	1.3e-6	34
Case 3	0.4917	120	3.3e-6	44.6	1.8e-5	49
Case 4	0.3008	42	1.7e-5	16.6	1.6e-4	16.7
Case 5	0.3303	52	1.2e-5	19.4	2.6e-4	21.5
Case 6	0.4611	66	5.4e-6	31.3	1.0e-4	31.5
Case 7	0.3683	97	5.5e-6	33.7	1.4e-5	42.5
Case 8	0.3495	62	6.2e-6	26.6	1.2e-5	28.7
Case 9	0.2911	86	1.5e-6	30.4	4.1e-5	32.2
Case 10	0.4083	121	2.0e-6	38.7	5.6e-5	52.9
Case 11	0.3180	44	2.9e-5	21.37	1.6e-4	25.3

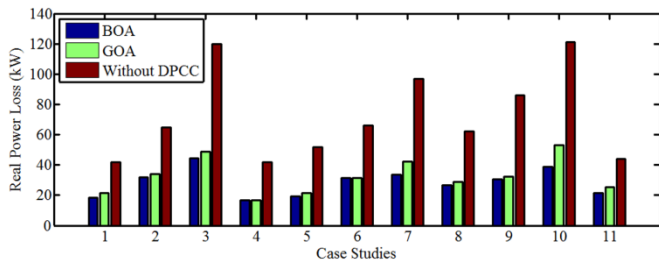


Figure 6 Comparison of the real power losses for different cases

As shown in Fig.6, in case 3, the real power losses decreased from an initial value of 120 kW down to 44.6 kW and 49 kW upon incorporating DPCC in the optimized position with optimized parameters gained by the BOA and GOA, respectively. When 40% overload is occurred in the MMG, after incorporating DPCC, the total real power losses are reduced significantly for both BOA (30.4 kW) and GOA (32.2 kW) methods. In all cases, MMG losses are decreased after incorporating DPCC and the BOA gives slightly better results than the GOA. Figures 7-13 show voltage distributions for the 33 bus MMG for different critical conditions.

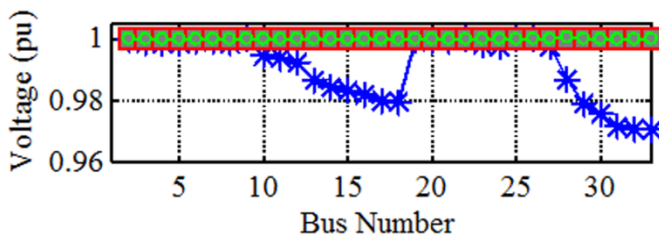


Figure 7. Voltage distributions in normal condition, star (*) (without DPCC), circle (●) (GOA), square (■) (BOA)

As shown in Fig.7, in the normal state, when the DPCC is not used across the studied MMG, 15 buses were deviated out of the desired voltage (1 pu) with a total bus voltage deviation of 0.2850 pu (Table 4). However, upon using the DPCC, all buses approached the desired value of 1 pu. Accordingly, the total bus voltage deviation dropped down to 0.000062 pu and 0.00059 pu when the BOA and GOA were used to solve the optimization problem, respectively.

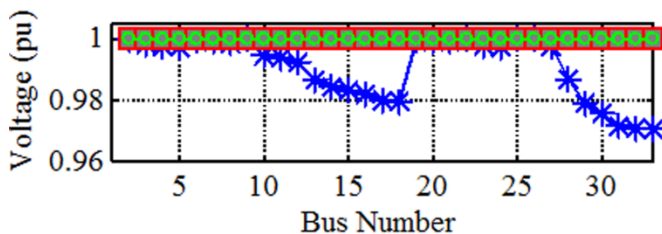
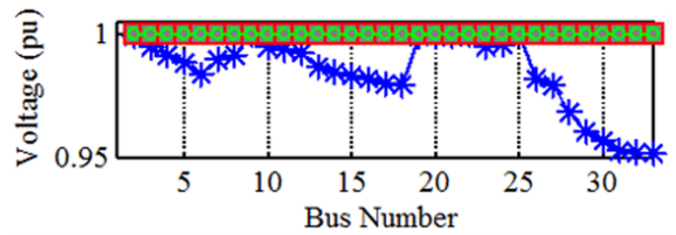


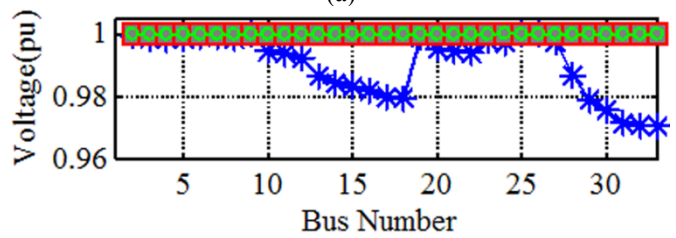
Figure 8. Voltage distributions when 50% generation reduced in DG1; star (*) (without DPCC), circle (●) (GOA), square (■) (BOA)

The relative capacity credit of renewable power plants is typically 25–50 percent. The generation reduction is expected in the MMGs that use renewable sources. Figure 8

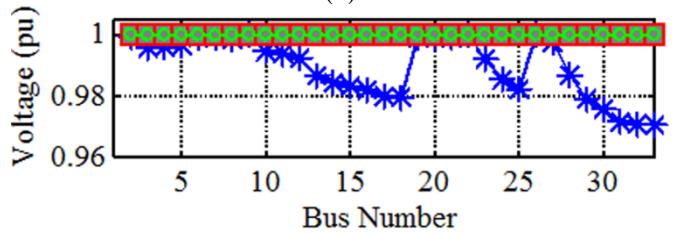
shows voltage distributions for the studied MMG when 50% generation reduced in DG1. After using the DPCC in the optimized position with the optimized parameters gained by the applied algorithms, all buses approached the desired value of 1 pu.



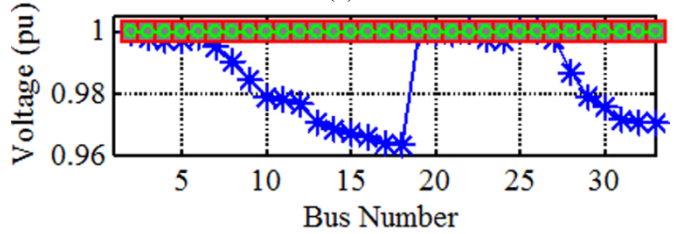
(a)



(b)



(c)



(d)

Figure 9. Voltage distributions when (a) DG1 outage (b) DG2 outage (c) DG3 outage (d) DG4 outage; star (*) (without DPCC), circle (●) (GOA), square (■) (BOA)

Figure 9 shows the voltage profile in MMG when the DGs are disconnected from each MG. For example, when the DG1 be lost in MG1, 25 buses were faced fluctuation voltage as shown in Fig.9(a). Also, the buses 30, 31, 32 and 33 were severely fluctuating that the fluctuations were eliminated after using DPCC. Accordingly, the total bus voltage deviation dropped down from 0.4917 pu to 0.0000033 pu and 0.000018 pu in this case when the BOA and GOA were used to solve the optimization problem, respectively. In all cases, after incorporating DPCC, the total voltage deviation is reduced significantly for both BOA and GOA methods as indicated in Table 4.

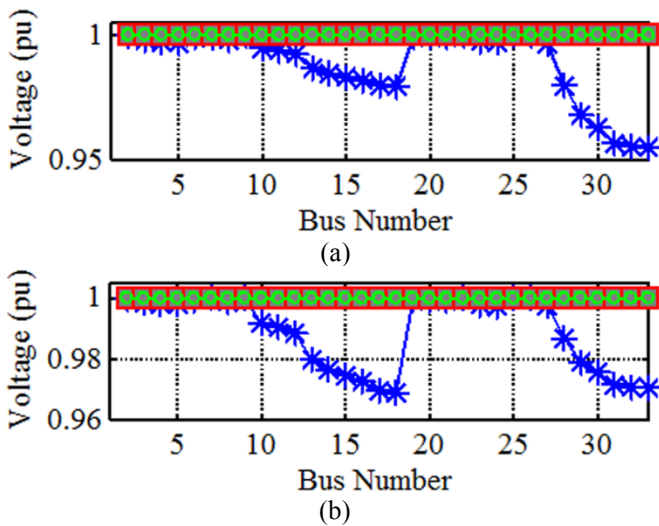


Figure 10. Voltage distributions when 50% overload occurred in (a) MG1 (b) MG4; star (*) (without DPCC), circle (●) (GOA), square (■) (BOA)

Figure 10 shows voltage distributions for the studied MMG, when 50% overload is occurred in the MG1 and MG4. As shown in Fig.10, the buses experienced the worst condition when MG1 was overloaded at 50%. The total voltage deviation decreased from an initial value of 0.3683 pu down to 0.0000055 pu and 0.000014 pu upon incorporating DPCC when the BOA and GOA were used to solve the optimization problem, respectively. In both cases, after incorporating DPCC, the total voltage deviation is reduced significantly for both GOA and BOA methods as indicated in Table 4.

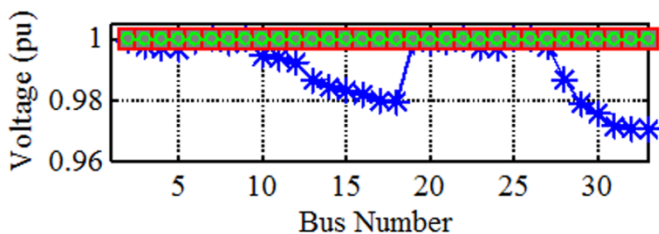


Figure 11. Voltage distributions when 40 % generation reduced in the MMG; star (*) (without DPCC), circle (●) (GOA), square (■) (BOA)

When generation reduces in the MMG, voltages at some buses were deviated out of the desired voltage as shown in Fig.11. After using the DPCC, all buses approached the desired value of 1 pu in all cases. The generation reduction is expected in the MMGs that use renewable sources.

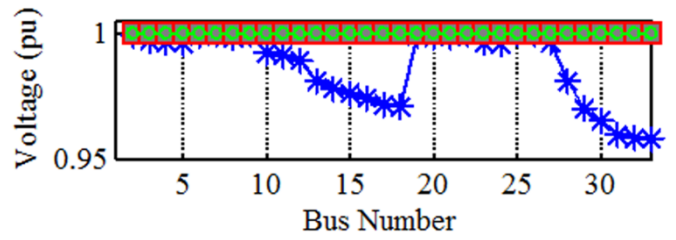


Figure 12. Voltage distributions when 40 % overload occurred in the MMG; star (*) (without DPCC), circle (●) (GOA), square (■) (BOA)

As shown in Fig.12, the buses experienced the worst condition when the studied MMG was overloaded at 40%. In such a case, 19 buses were deviated out of the desired voltage (1 pu), with three of them (the buses 31, 32 and 33) been severely deviated out of range. After using the DPCC, all buses approached the desired value of 1 pu.

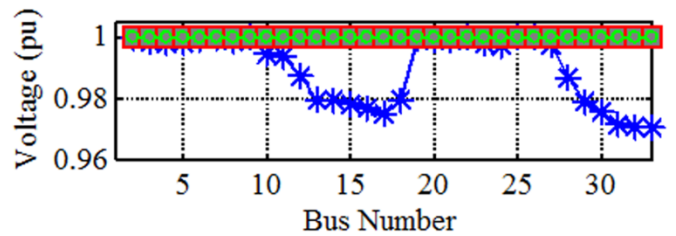


Figure 13. Voltage distributions when line contingency occurred in the MMG; star (*) (without DPCC), circle (●) (GOA), square (■) (BOA)

Figure 13 shows voltage distributions when line contingency occurs on the MMG. When line between buses 12 and 22 is outage, 18 buses were deviated out of the desired voltage (1 pu) with a total bus voltage deviation of 0.3180 pu (Table 4). However, upon using the DPCC, all buses approached the desired value of 1 pu. Accordingly, the total bus voltage deviation dropped down to .000029 pu and 0.00016 pu when the BOA and GOA were used to solve the optimization problem, respectively.

As presented in Figs. 7-13, both of the optimization algorithms demonstrated the effectiveness of using the DPCC with optimal parameters at appropriate position across the MMG for regulating the voltage and decreasing the losses. The results further indicated the slightly superiority of the BOA over the GOA for such a purpose.

From the simulation results indicated in Table 3, it is clear that line 27-28 is the optimal location that is frequently acquired in all case studies for DPCC installation. Now, it is assumed that the DPCC is installed on line 27-28, its performance in voltage regulation and loss reduction is investigated only by setting the series and shunt voltage control parameters in uncertainty and critical cases occurred in MMG. The results obtained by the BOA are listed in Table 5.

Table 5. The DPCC performance in voltage regulation and loss reduction of MMG in critical cases

Results obtained by the BOA	Case studies		Without DPCC		With DPCC			
			$F1$	$F2$	$F1$	$F2$	V_{ser}	V_{sh}
Uncertainty and critical situations in MG1	50%	Overload in MG1	0.37	97	9.6e-6	40.3	0.03641	0.95338
	100%		0.46	235	6.3e-5	103.7	0.03634	0.93803
	50%	Generation reduction in DG1	0.29	65	4.3e-7	31.7	0.03656	0.9845
	75%		0.29	102	2.6e-5	41.3	0.03636	0.94396
	DG1 outage		0.49	120	7.5e-5	49.4	0.03635	0.94081
Uncertainty and critical situations in MG2	50%	Overload in MG2	0.29	42	3.4e-6	27	0.03634	0.93687
	100%		0.29	42	3.7e-5	21.8	0.03636	0.94244
	50%	Generation reduction in DG2	0.29	42	8.6e-7	16.1	0.03654	0.97979
	75%		0.29	42	3.7e-5	22.3	0.03636	0.94244
	DG2 outage		0.30	42	1.7e-5	16.6	0.03669	1.0058
Uncertainty and critical situations in MG3	50%	Overload in MG3	0.29	42	1.2e-5	18.4	0.03637	0.94515
	100%		0.30	56	1.2e-5	26.6	0.03654	0.98163
	50%	Generation reduction in DG3	0.29	42	1.7e-6	19.3	0.03626	0.91167
	75%		0.29	52	9.7e-6	24.3	0.03644	0.96141
	DG3 outage		0.33	52	1.2e-5	19.4	0.03649	0.9712
Uncertainty and critical situations in MG4	50%	Overload in MG4	0.35	62	6.2e-6	26.6	0.0364	0.9523
	100%		0.42	107	1.1e-4	46.7	0.03673	1.0102
	50%	Generation reduction in DG4	0.29	51	6.2e-6	22.4	0.0364	0.95229
	75%		0.29	63	3.4e-6	27	0.03634	0.93686
	DG4 outage		0.46	66	5.4e-6	31.3	0.03643	0.95991
Critical situations in MMG	20%	Generation reduction	0.29	47	4.2e-5	22.2	0.03672	1.00932
	40%		0.29	86	6.1e-5	38.4	0.03642	0.95494
	20%	Overload in MMG	0.35	64	4.2e-5	29.3	0.03662	0.99451
	40%		0.41	121	2.0e-6	38.7	0.03652	0.977
line contingency	line 12-22 outage		0.3180	44	2.9e-5	21.37	0.0364	0.9345

The reference control voltage of DPCC for the converters is transmitted by the central control by sensing local situation. With appropriate control plan, series and shunt voltage in DPCC can be adjusted according to different situations. As shown in Table 5, the voltage profile at all buses have been improved significantly, after using DPCC with optimal parameters.

5. Conclusion

When a critical situation such as generation reduction because of the intermittent nature of renewable energy sources, DG outage in each MG, overload or line contingency occurs in the MMG, the voltages at some buses fluctuate more than the allowed level and power loss arises which is harmful to vital applications. In this paper optimal placement and parameter tuning of DPCC for enhancing the voltage profile and reducing losses in a sample isolated MMG under critical situations with two high-performing optimization algorithms have been investigated. It is found from theory studies and simulation results that the DPCC has high capability to control bus voltages and reduce losses in the MMG considering capacity credit of the renewable power plants and optimal placement and parameter tuning of the DPCC successfully improve the MMG performance. After using DPCC in the best location with optimal parameters, the real power losses of the MMG have been lessened significantly and the voltage profile at all buses has been improved in all critical situations. The result shows both of

BOA and GOA are powerful optimization techniques that can find the optimal values with very high accuracy and BOA gives slightly outcomes compared to GOA.

References

- [1] A. Safari, F. Babaei, M. Farrokhifar, "A load frequency control using a PSO-based ANN for micro-grids in the presence of electric vehicles", *International Journal of Ambient Energy*, pp. 1-13, 2019.
- [2] S. Abderrahim, M. Allouche, M. Chaabane, "A New Robust Control Strategy for a Wind Energy Conversion System Based on a TS Fuzzy Model", *International Journal of Smart Grid*, vol. 4, pp. 88-99, 2020.
- [3] M. Esmaili, H. Shayeghi, M. Nooshyar, H. Aryanpour, "Design of new controller for load frequency control of isolated microgrid considering system uncertainties", *International Journal of Power and Energy Conversion*, vol. 9, pp. 285-294, 2018.
- [4] M. Monadi, H. Farzin, P. Rodriguez, "A Distributed Self-Healing Method for Active Distribution Systems", in *2019 8th International Conference on Renewable Energy Research and Applications*, 2019, pp. 483-488.
- [5] H Zou, Sh Mao, Y Wang, F Zhang, X Chen, L Cheng, "A survey of energy management in interconnected multi-microgrids", *IEEE Access*, vol. 7, pp. 72158-72169, 2019.
- [6] Y Kobayashi, M Hamanaka, K Niimi, K Yukita, T Matsumura, Y Goto, "Power Quality Improvement

- Method Using EV for PV Output Fluctuation," in 2018 International Conference on Smart Grid, 2018, pp. 272-275.
- [7] N. Bayati, H. R. Baghaee, A. Hajizadeh, M. Soltani, "Localized Protection of Radial DC Microgrids With High Penetration of Constant Power Loads," *IEEE Systems Journal*, 2020.
- [8] A. Bouhouta, S. Moulahoum, N. Kabache, I. Colak, "Experimental Investigation of Fuzzy Logic Controller Based Indirect Current Control Algorithm for Shunt Active Power Filter", in 2019 8th International Conference on Renewable Energy Research and Applications, 2019, pp. 309-314.
- [9] T. Amare, C. M. Adrah, B. E. Helvik, "A Method for Performability Study on Wide Area Communication Architectures for Smart Grid," in 2019 7th International Conference on Smart Grid, 2019, pp. 64-73.
- [10] F. Aghaee, N. Mahdian Dehkordi, N. Bayati, A. Hajizadeh, "Distributed control methods and impact of communication failure in AC microgrids: A comparative review", *Electronics*, vol. 8, p. 1265, 2019.
- [11] S. Samal and P. K. Hota, "Power quality improvement by solar photo-voltaic/fuel cell Integrated system using unified power quality conditioner", *International Journal of Renewable Energy Research*, vol. 7, pp. 2075-2084, 2017.
- [12] K. Behzadpour and M. R. Amini, "Applying a Novel Soft Switching Technique to Three-Phase Active Power Filter", in 2019 8th International Conference on Renewable Energy Research and Applications, 2019, pp. 563-567.
- [13] T. S. Saggi, L. Singh, B. Gill, "Harmonics mitigation in a steel industry using 11-level cascaded multilevel inverter-based dstatcom", *Canadian Journal of Electrical and Computer Engineering*, vol. 40, pp. 110-115, 2017.
- [14] S. A. Taher and S. A. Afsari, "Optimal location and sizing of DSTATCOM in distribution systems by immune algorithm", *International Journal of Electrical Power & Energy Systems*, vol. 60, pp. 34-44, 2014.
- [15] F. Iqbal, M. T. Khan, A. S. Siddiqui, "Optimal placement of DG and DSTATCOM for loss reduction and voltage profile improvement", *Alexandria Engineering Journal*, vol. 57, pp. 755-765, 2018.
- [16] A. Lakum and V. Mahajan, "Optimal placement and sizing of multiple active power filters in radial distribution system using grey wolf optimizer in presence of nonlinear distributed generation", *Electric Power Systems Research*, vol. 173, pp. 281-290, 2019.
- [17] M. Moghbel, M. A. Masoum, A. Fereidouni, S. Deilami, "Optimal sizing, siting and operation of custom power devices with STATCOM and APLC functions for real-time reactive power and network voltage quality control of smart grid", *IEEE Transactions on Smart Grid*, vol. 9, pp. 5564-5575, 2017.
- [18] Y. Li, B. Feng, G. Li, J. Qi, D. Zhao, Y. Mu, "Optimal distributed generation planning in active distribution networks considering integration of energy storage", *Applied Energy*, vol. 210, pp. 1073-1081, 2018.
- [19] J. Sarker and S. Goswami, "Optimal location of unified power quality conditioner in distribution system for power quality improvement", *International Journal of Electrical Power & Energy Systems*, vol. 83, pp. 309-324, 2016.
- [20] M. Esmaeili, H. Shayeghi, K. Valipour, A. Safari, F. Sedaghati, "Power quality improvement of multimicrogrid using improved custom power device called as distributed power condition controller", *International Transactions on Electrical Energy Systems*, vol. 30, p. e12259, 2020.
- [21] S. Arora and S. Singh, "Butterfly optimization algorithm: a novel approach for global optimization", *Soft Computing*, vol. 23, pp. 715-734, 2019.
- [22] S. Saremi, S. Mirjalili, A. Lewis, "Grasshopper optimization algorithm: theory and application", *Advances in Engineering Software*, vol. 105, pp. 30-47, 2017.
- [23] H. Moazami Goodarzi and M. H. Kazemi, "A novel optimal control method for islanded microgrids based on droop control using the ICA-GA algorithm", *Energies*, vol. 10, pp. 485, 2017.